

DESIGN AND DEVELOPMENT OF NON-ISOLATED THREE PORT BIDIRECTIONAL BOOST+CUK DC-DC CONVERTER FOR ELECTRIC VEHICLES

Balasubramanian.S¹, Adithya.S², Sre Vignesh.S³, Balaji.C⁴

^{1,2,3}Department of EEE, SRM Institute of Science and Technology, Kattankulathur – 603 203, Kancheepuram Dt., Tamil Nadu, India

¹Balasubramanian_sendilcoumar@srmuniv.edu.in

²Adithya_srinivasan@srmuniv.edu.in

³Srevignesh_saravanan@srmuniv.edu.in

⁴Assistant Professor, Dept. of EEE, SRM Institute of Science and Technology, Kattankulathur - 603203, Kancheepuram Dt., Tamil Nadu, India

⁴balaji2work@gmail.com

ABSTRACT: A large number of conventional vehicles in use around the world has caused and continues to cause serious environmental hazards like pollution and resource depletion which in turn has affected humans and other forms. Electric Vehicles (EVs), Hybrid Electric Vehicles (HEVs) and Fuel Cell Electric Vehicles (FCEVs) have been typically proposed to replace conventional vehicles soon as a solution to the problem. This paper proposes a novel non-isolated three-port bidirectional boost-cuk (NI-TPBBC) DC-DC converter for electric vehicle applications. The proposed converter combines the characteristics of Boost and Cuk converters, providing five viable modes of operation along with provision for regenerative energy utilization. The converter is compatible with the use of two input sources. The proposed converter is extensively studied and the simulated results are carried to verify their viability for practical use.

KEYWORDS: Bidirectional DC-DC Converter, Non-isolated converter, Boost and Cuk converter, Multiport Converter, High-voltage gain, electric vehicle application.

I. INTRODUCTION

Renewable energy sources play an important role in the present energy scenario in spite of having low voltage characteristics. Therefore, for practical applications, a high voltage gain and high-efficiency DC-DC converters are necessary to control the characteristics of the low voltage into a utilization voltage level.

Bidirectional DC-DC converters can implement the electrical energies of the storage units (batteries/capacitors) to be converted and transferred in two directions thereby providing flexibility and possible integration of renewable energy by providing more than one port as input energy. The voltage of the storage units is set to be low and the DC link voltage between the sources and application(DC motor) is set to be high. Hence, a bidirectional converter that can operate in both boost and buck modes is crucial to obtain voltage matching.

In this scenario, the requirement of a bidirectional DC-DC converter with high efficiency and conversion ratio is still an area of research interest in the power electronics field.

The proposed converter attempts to meet the required converter model. The converter operates in bidirectional mode with a high voltage conversion ratio and a reduced number of active components complying with reduced loss and higher efficiency setting.

It has five modes of operation which are extensively studied and experimented upon for practical viability. A prototype is built to validate the calculated values. The converter also gives the provision of two input ports making it compatible with renewable energy applications such as electric vehicles.

II. TOPOLOGY OF THE PROPOSED CONVERTER

The proposed converter (Figure 1) consists of two inputs namely a PV source and battery. The configuration is based on the integration of a Boost converter with a Cuk converter. The boost and buck static gain of these types of converters are beneficial features for wide range voltage conversion. Power flow is bidirectional in the new converter.

The converter consists of a branch network to compensate two input modes and the Boost-Cuk circuit. The supply network employs switch T to control power flow from the PV source.

The supply network consists of three IGBTs, an inductor, and a relay R_s to manipulate the power to the Boost network. The supply branch provides the necessary topology for battery discharging and charging through PV supply as well as a path for regenerative power to charge the battery.

The Boost-Cuk circuit consists of three power switches $S1$, $S2$, and $S3$; capacitors $C1$, $C2$, and $C3$; and inductors $L1$ and $L2$. The proposed topology is achieved by developing [7]. The bidirectional setting is achieved by modifying the circuit to the required specification. The proposed converter is examined on the assumption that it operates in continuous conduction mode (CCM), and that all the components are ideal.

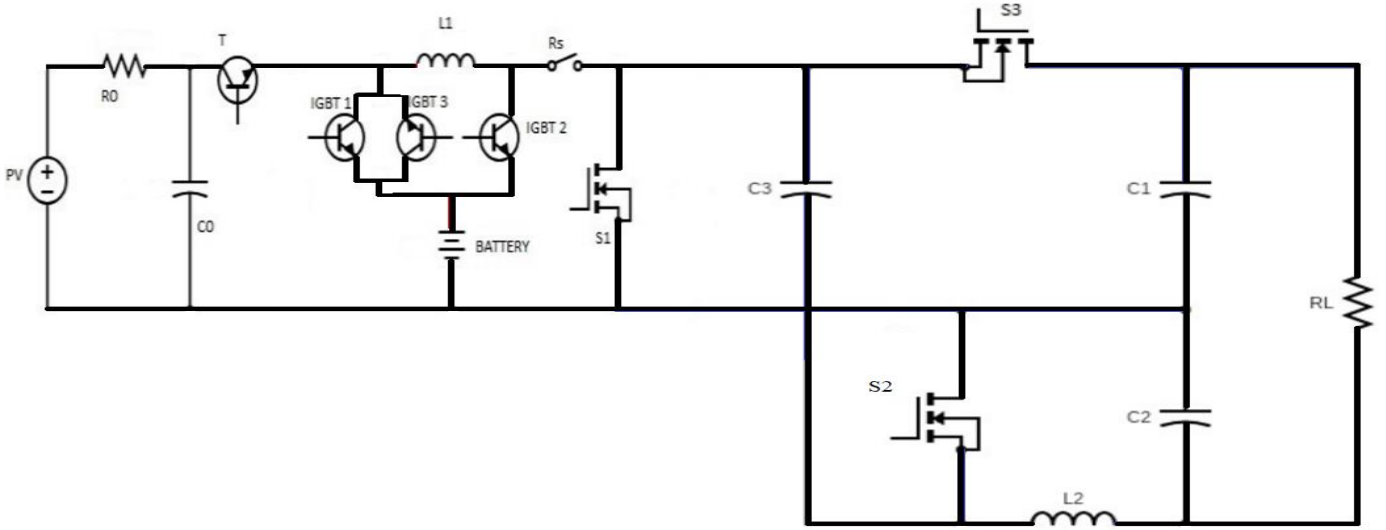


Figure 1 Topology of the Proposed Converter

III. OPERATIONAL MODES

1. PV Supply to Load (SISO – 1)

In this mode, the PV supplies to the load. The battery circuit is detached from the network by opening switches $IGBT 1$, $IGBT 2$ and $IGBT 3$. The switch T is turned ON along with the relay R_s . Two sub-modes arise due to the switching operation of switch $S1$. During ON State (Figure 2a), the Switch $S1$ is ON. At this period, the current from PV source flows through Switches T and $S1$ thereby completing the current path. The Inductor $L1$ charges at this period. Capacitor $C3$ discharges through switch $S1$. Capacitor current branches into two components.

The switches $S2$ and $S3$ are reverse biased.

This is because the voltage across capacitor $C1$ is greater than that of across capacitor $C3$. Capacitor $C1$ discharges and supplies to the load. Capacitor $C2$ charges at this period. The inductor $L2$ charges and the current path is completed.

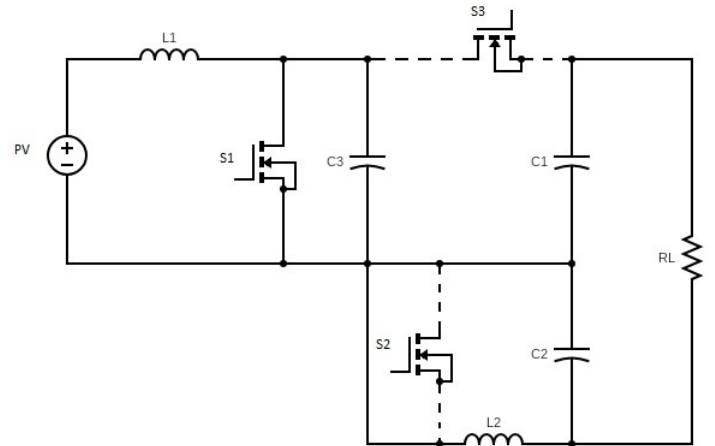


Figure 2a ON State (Switch $S1$ - ON, $S2, S3$ - OFF) – Mode 1

During the OFF state of switch S_1 (Figures 2b - 2c), there arise two scenarios. When the voltage across capacitor C_1 is greater than the voltage across capacitor C_3 ($V_{c1} > V_{c3}$), the inductor L_1 current discharges through the relay R_s . Capacitor C_3 charges. Switch S_2 is forward biased. Inductor L_2 discharges through diode S_2 and charges the capacitor C_2 . The capacitor C_1 discharges feeding the load.

When the voltage across capacitor C_3 is greater than the voltage across capacitor C_1 ($V_{c3} > V_{c1}$), the inductor L_1 continues to discharge. Due to the charging of capacitor C_3 , the voltage builds up and increases to more than that across capacitor C_1 . Hence, switch S_3 is forward biased. The capacitors C_1 and C_3 are charged. Capacitor C_2 discharges. Inductor L_2 discharges through diode S_2 .

Table 1 Switching Chart for Mode 1

MODE (Switch S_1)	R_s	S_1	S_2	S_3
ON	1	1	0	0
OFF ($V_{c1} > V_{c3}$)	1	0	1	0
OFF ($V_{c3} > V_{c1}$)	1	0	1	1

Table 1 shows the switching sequence employed in each state.

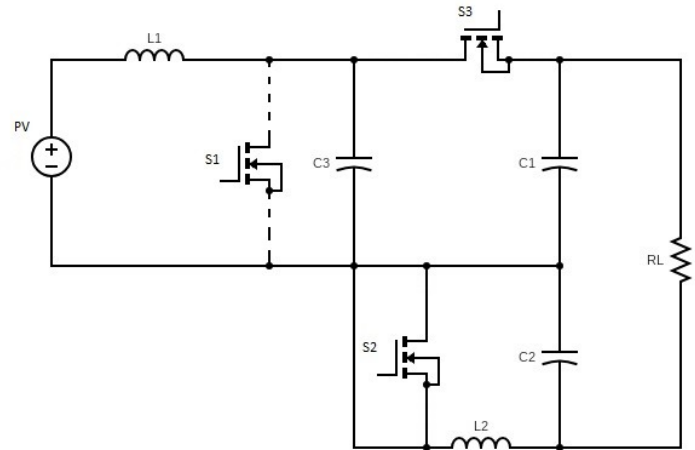


Figure 2c OFF State ($V_{c1} > V_{c3}$) (Switch S_2, S_3 – ON, S_1 – OFF) – Mode 2

2. Battery to Load (SISO – 2)

In this mode, the battery supplies to the load. It is similar to Mode 1. The PV circuit is detached from the network by opening switch T . The switch $IGBT_3$ is turned ON along with the relay R_s .

During ON State (figure 3a), the Switch S_1 is ON. At this period, the current from the battery flows through Switches T and S_1 thereby completing the Current path. The Inductor L_1 charges at this period. Capacitor C_3 discharges through switch S_1 . It branches into two components. The switches S_2 and S_3 are reverse biased. This is because the voltage across C_1 is greater than that of across C_3 . Capacitor C_1 discharges and supplies to the load. Capacitor C_2 charges at this period. The inductor L_2 charges and the current path is completed.

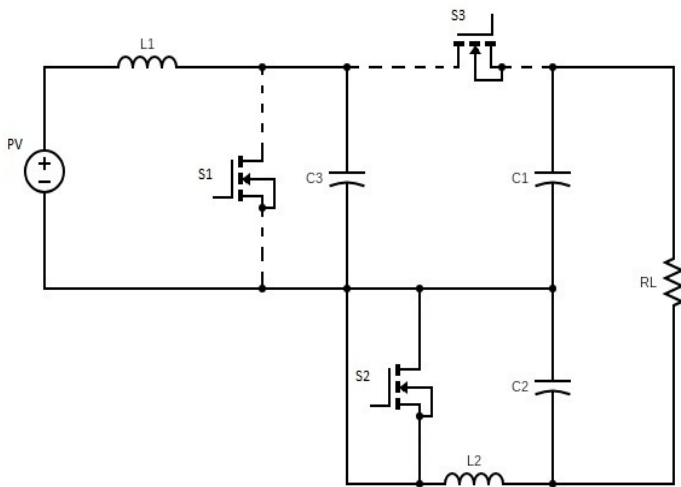


Figure 2b OFF State ($V_{c1} > V_{c3}$) (Switch S_1, S_3 – OFF, S_2 – ON) – Mode 2

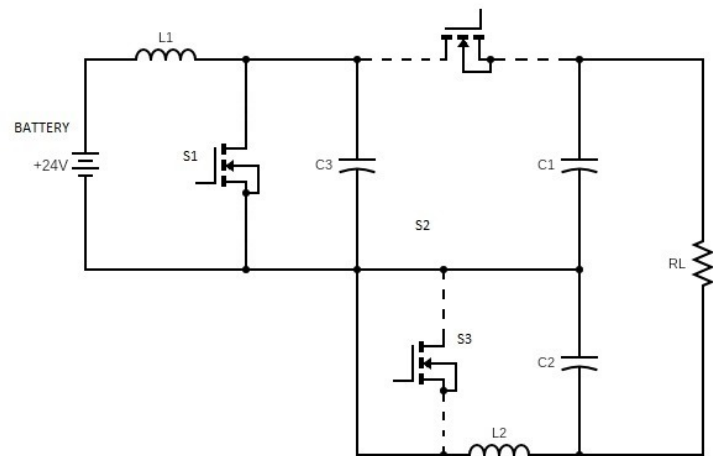


Figure 3a ON State (Switch S_1 – ON, S_2, S_3 – OFF) – Mode 2

During the OFF state (figure 3b – 3c), there arise two scenarios. When the voltage across capacitor $C1$ is greater than the voltage across capacitor $C3$ ($V_{c1} > V_{c3}$), the inductor $L1$ discharges through the relay. Switch $S1$ is OFF. Capacitor $C3$ charges. Switch $S2$ is forward biased. Inductor $L2$ discharges through switch $S2$ and charges the capacitor $C2$. The capacitor $C1$ discharges feeding the load.

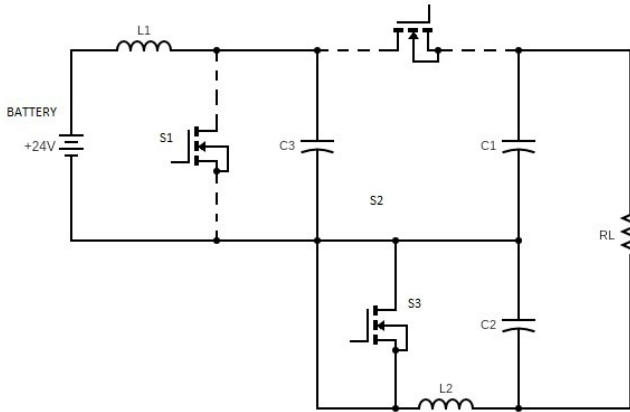


Figure 3b OFF State ($V_{c1} > V_{c3}$) (Switch $S1, S3$ – OFF, $S2$ – ON) – Mode 2

When the voltage across capacitor $C3$ is greater than the voltage across capacitor $C1$ ($V_{c3} > V_{c1}$), the inductor $L1$ continues to discharge. Due to the charging of capacitor $C3$, the voltage builds up and increases to more than that across capacitor $C1$. Hence, diode $S3$ is forward biased. The capacitors $C1$ and $C3$ are charged. Capacitor $C2$ discharges. Inductor $L2$ discharges through diode $S2$.

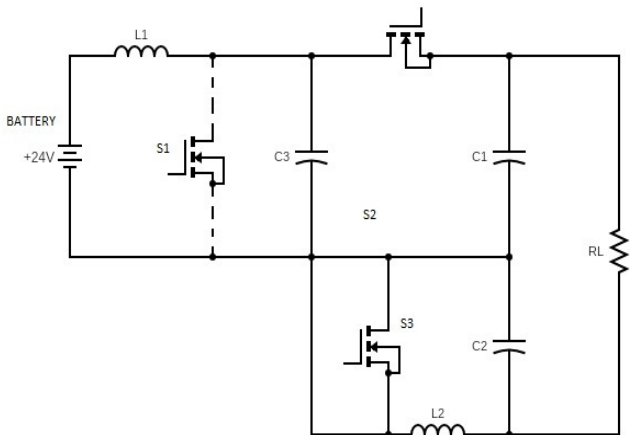


Figure 3c OFF State ($V_{c3} > V_{c1}$) (Switch $S2, S3$ – ON, $S1$ – OFF) – Mode 2

Table 2 Switching Chart for Mode 2

MODE	T	IGBT ₁	IGBT ₂	IGBT ₃	R _s	S ₁	S ₂	S ₃
ON	0	0	0	1	1	1	0	0
OFF($V_{c1} > V_{c3}$)	0	0	0	1	1	0	1	0
OFF($V_{c3} > V_{c1}$)	0	0	0	1	1	0	1	1

3. PV Supply and Battery to Load (DISO)

During peak load requirement i.e when the electric vehicle is in operation and requires power more than the average operating power requirement, there arises a need for both the primary and the secondary source to supply the traction system. Also, the supply from PV and BATTERY are alternated based on the availability of PV energy and the energy required by the load.

During the first cycle of operation ($0 - t_1$), PV supply is used to cater to the load. In the next cycle of operation ($t_1 - t_2$), PV supply is removed by opening switch T, and battery supply is included by closing IGBT3. The load sharing is controlled using the duty cycle of the control switch T and IGBT3. The two sub-modes are:

1) PV to LOAD 2) BATTERY TO LOAD

During each of the above modes, the switching operation corresponding to each of the individual modes is performed in their respective period of operation, thus the operational characteristics mentioned in (1) and (2) hold good in this mode.

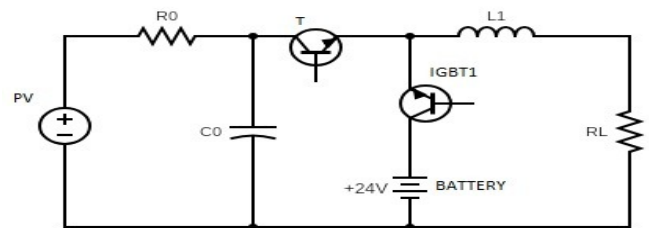


Figure 4 Mode 3 Operation

Table 3 Switching Chart for Mode 3

CONDITION	MODE	T	IGBT ₁	IGBT ₂	IGBT ₃	R _s	S ₁	S ₂	S ₃
PV Supply	ON	1	0	0	0	1	1	0	0
	OFF($V_{c1} > V_{c3}$)	1	0	0	0	1	0	1	0
	OFF($V_{c3} > V_{c1}$)	1	0	0	0	1	0	1	1
Battery	ON	0	0	0	1	1	1	0	0
	OFF($V_{c1} > V_{c3}$)	0	0	0	1	1	0	1	0
	OFF($V_{c3} > V_{c1}$)	0	0	0	1	1	0	1	1

4. Regenerative Braking (SISO – 3)

The regenerative braking action is executed by using the pressure inserted onto the brake levers during the regular braking action to convert the motoring action of the traction system into an intermittent generating action, wherein the voltage produced by the generating action of the traction system, is fed to the battery by the buck operation of the converter.

Whenever the braking action takes place, the traction motor temporarily shifts to generating action, thus producing a current flow into the circuit. This is where the Bi-directionality of the converter comes into use. The Switch T and switch B_s are in Off state. Thus current flows through the inductor $L1$ thereby charging it. IGBT2 and IGBT3 are in OFF state, thus the current produced from the braking action is fed to the battery through the IGBT1.

Table 4 Switching Chart for Mode 4

IGBT ₁	S ₁	S ₂	S ₃
1	1	0	0
1	0	1	1

Figure 5.21 shows the capacitor voltages, Inductor currents, and switching currents when the switches are operated in the above sequence.

5. PV to Battery

Apart from the above four modes of operation, there is a possibility to modify the converter design to accommodate one more operating mode.

To implement the operation of PV to Battery power flow, the need to add additional switches to the proposed design arises. Hence switch “Bs” is added for this mode of operation. The stationary phase of the EV is when the battery gets charged to cater to the demand in the recurring operational modes.

During this time, the PV source has to feed the energy storage systems through the converter as a buck operation is to be executed for the same. In the initial cycle of operation, the Switch T is closed. Hence the power arriving from the PV source charges the Inductor and feeds the battery through the IGBT2 thereby completing the current flow. During this mode, the switch B_s is in the OFF state.

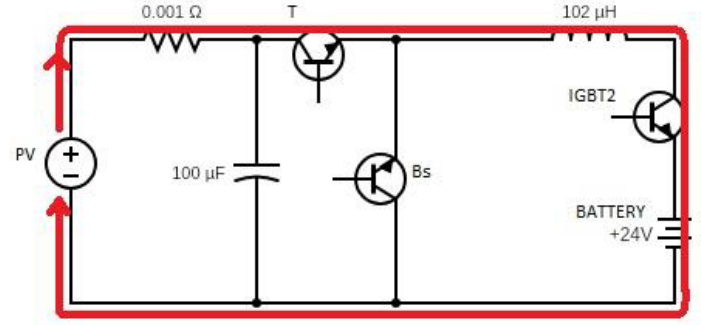


Figure 4a PV to Battery State – 1

During the second cycle of operation, the switch T is now opened and the Switch B_s is closed, thereby moving into ON state. The inductor which was charged in the previous cycle, now discharges through the IGBT2, thereby charging the energy storage system.

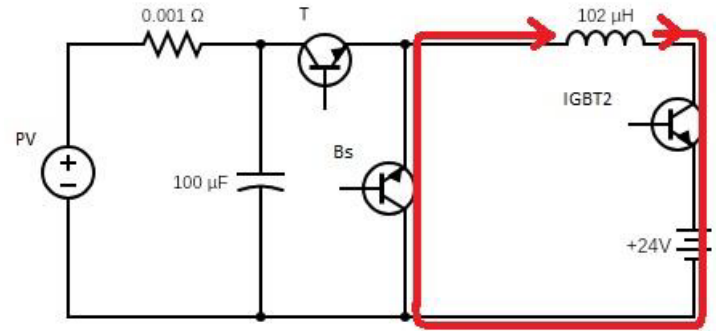


Figure 4b PV to Battery State – 2

Table 5 Switching Chart for Mode 5

Mode (Switch T)	Bs	IGBT 2
1	0	1
0	1	1

IV. VOLTAGE GAIN EQUATION

By applying the volt-second balance equation to $L1$ and $L2$ according to Fig.7, the voltage gain V_g of the proposed NI-TPBBC converter in CCM can be obtained as:

$$\frac{1}{T} \int_0^T v_L(t) dt = 0$$

By substituting the inductor (L_1, L_2) equations:

$$\frac{1}{T} \int_0^d V_{in} dt + \frac{1}{T} \int_d^1 \frac{V_{in} - V_o}{2} dt = 0 \quad (1)$$

$$V_{in}d + \frac{1}{2}(V_{in} - V_o)(1 - d) = 0 \quad (2)$$

$$V_{in}d + V_{in} - V_o + V_o d = 0 \quad (3)$$

$$V_g = \frac{V_o}{V_{in}} = \frac{1 + d}{1 - d} \quad (4)$$

V. SOFTWARE AND HARDWARE ANALYSIS

The proposed and theorized converter model is simulated using Matlab software and the obtained results are matched with a 250 W laboratory prototype.

Table 6 Parameters

Component	Abbreviation	Rating
PV Supply	Vpv	40 V
Battery Pack	Vb	24 V
Inductors	L1-L2	100uH
Capacitors	C1-C2 C3	50uF 3.3uF
Switching Frequency	f_s	15kHz
Power Rating		250W

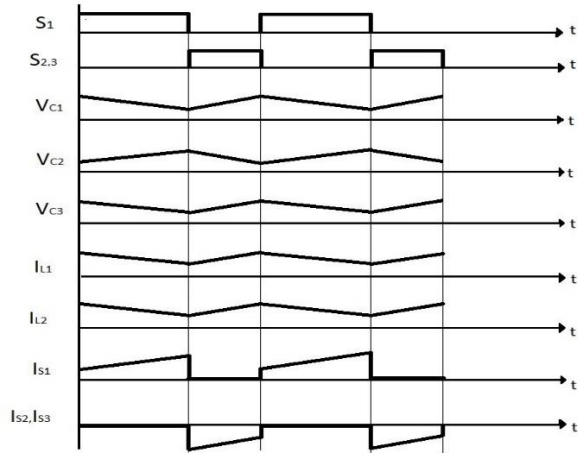


Figure 7 Principle Waveforms of proposed NI-TPBBC Converter; S_1, S_2, S_3 – Pulse period, V_{c1}, V_{c2}, V_{c3} – Capacitor Voltages, IL_1 – Inductor L_1 current, IL_2 – Inductor L_2 current, Is_1 – Switching current of S_1 , Is_2 – Switching current of S_2 , Is_3 – Switching current S_3

By applying the Kirchhoff voltage law on the proposed NI-TPBBC converter, the voltage stress can be obtained as:

$$V_{s1,s2,s3} = \frac{V_{in}}{1 - d}$$

Similarly, by applying the Kirchhoff current law, the current stress can be expressed as follows:

$$I_{s1} = \frac{2}{1 - d} I_{in}$$

$$I_{s2,s3} = \frac{1}{1 - d} I_{in}$$

Where “d” is the duty cycle of switching.

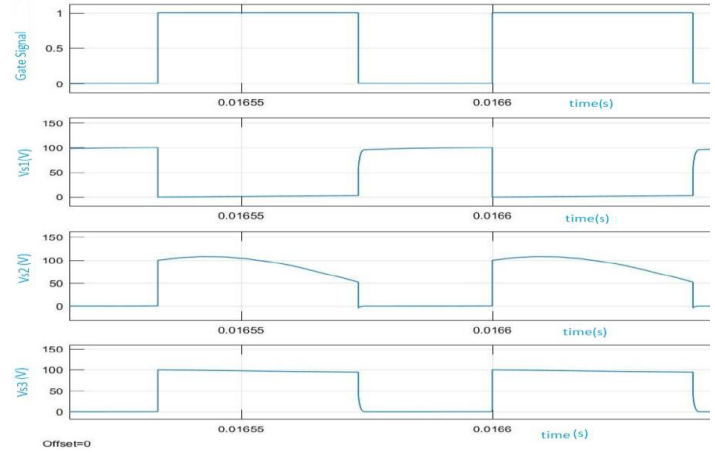


Figure 5 Voltage Stress on Switches

Figure 5 shows the voltage stress on switches S_1, S_2 , and S_3 . It is observed that when S_1 is in OFF condition, a maximum of around 97 V appears across it.

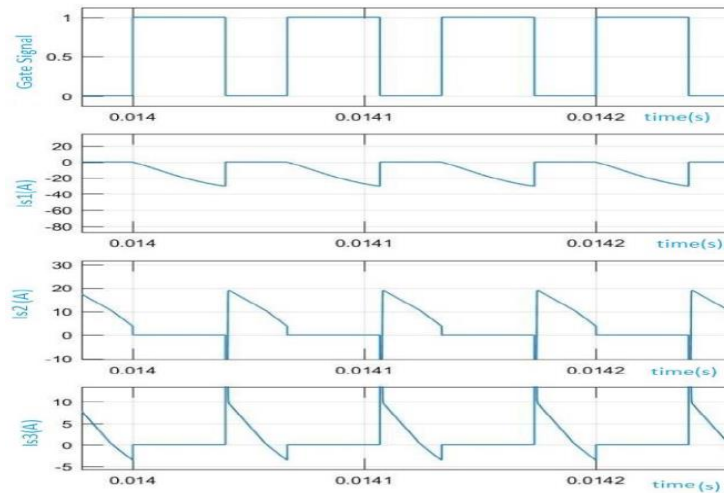
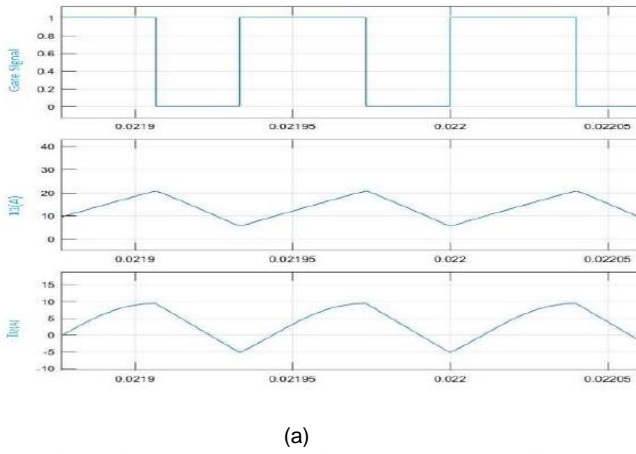


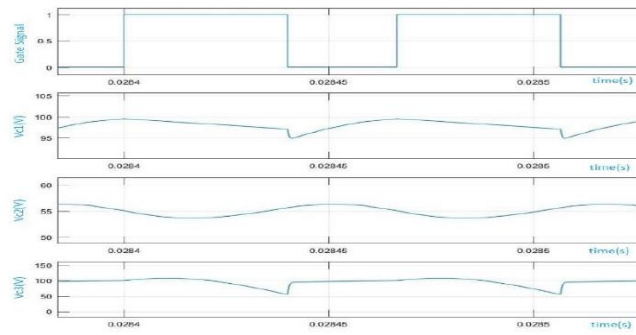
Figure 6 Current Stress on Switches

Figure 6 shows the current stress across switches S1, S2, and S3. It is observed that when S1 is in ON condition, a maximum of 30 A appears in it.

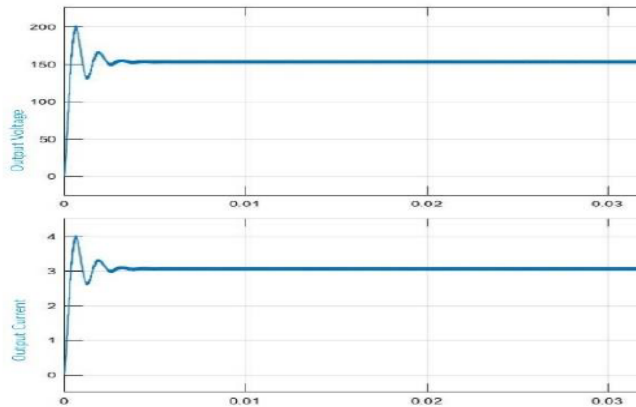
With the above-mentioned parameters, experimental results for the proposed NI-TPBBC Converter are obtained as in Figure 6.



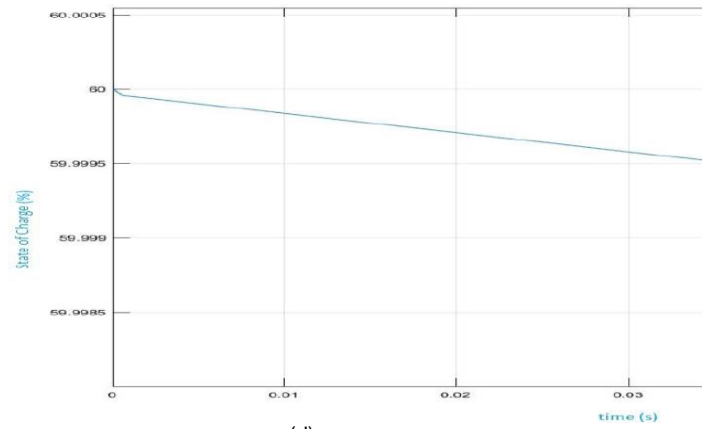
(a)



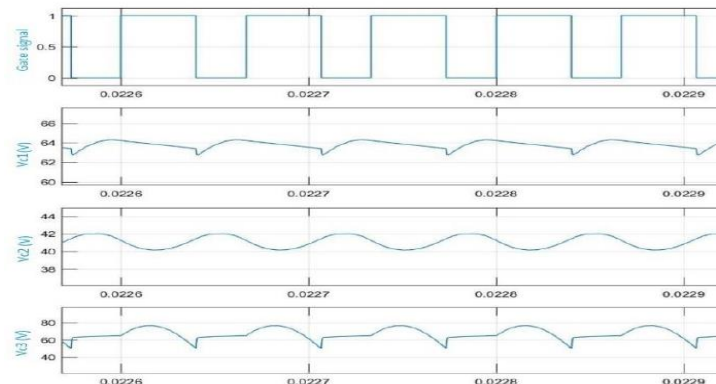
(b)



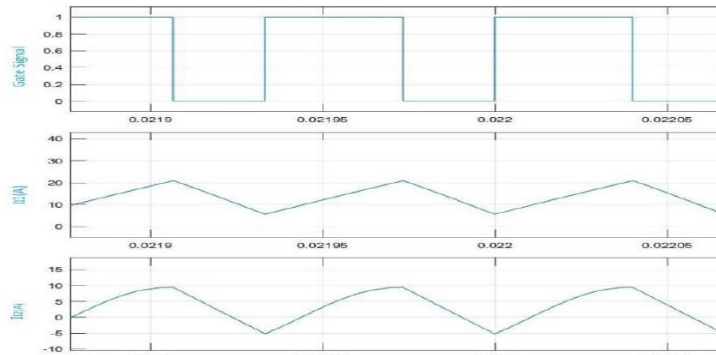
(c)



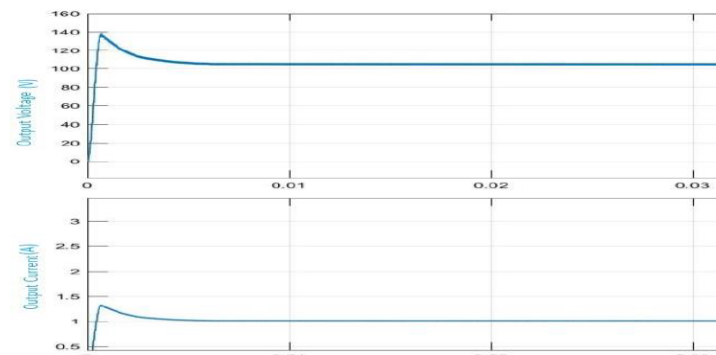
(d)



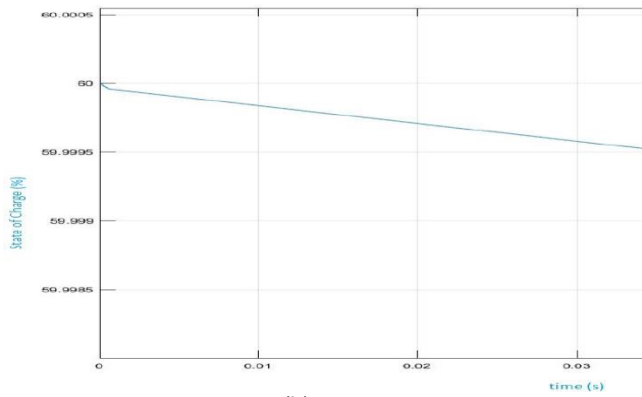
(e)



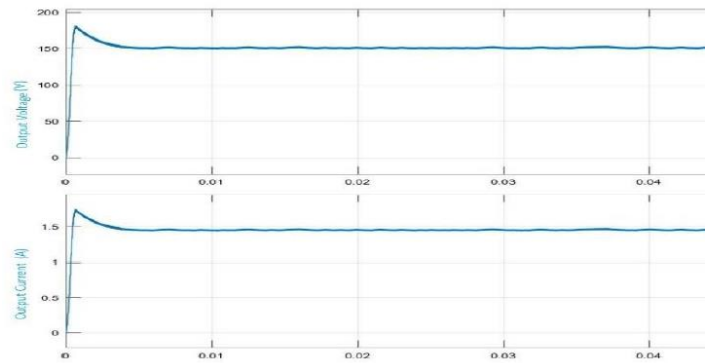
(f)



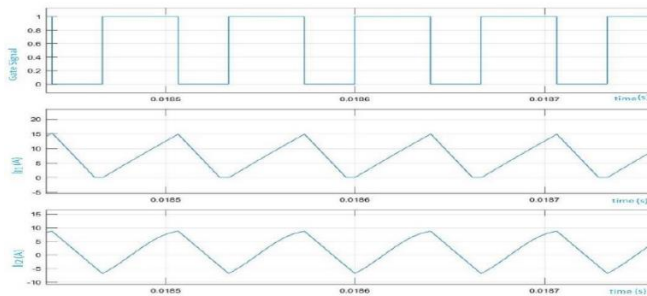
(g)



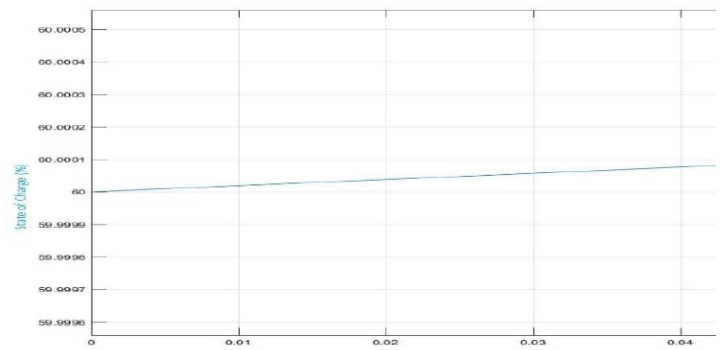
(h)



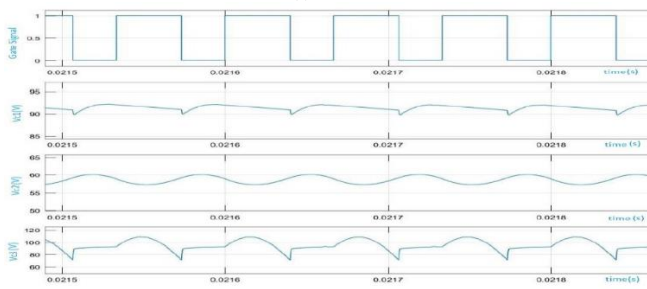
(k)



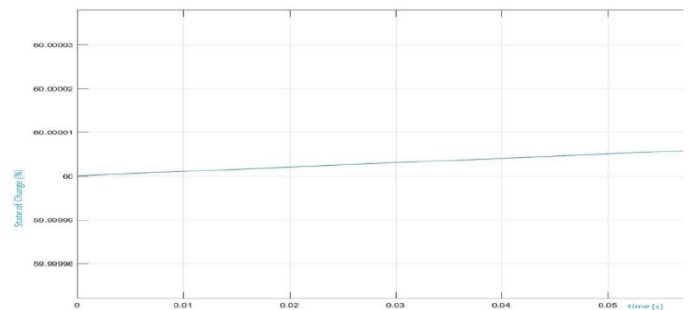
(i)



(l)



(j)



(m)

Figure 7 (a) Inductor Currents – PV to Load, (b) Capacitor Voltages – PV to Load, (c) Load Voltage and Load Current-PV to Load (d) Battery Condition – Battery to Load, (e) Capacitor Voltages – Battery to Load, (f) Inductor Currents – Battery to Load, (g) Load Voltage and Load Current-Battery to Load (h) Battery Condition – PV and Battery to Load, (i) Inductor Currents – PV and Battery to Load, (j) Capacitor Voltages – PV and Battery to Load, (k) Load Voltage and Load Current-PV and Battery to Load, (l) Battery Condition-Regenerative Braking, (m) Battery Condition-PV to Battery.

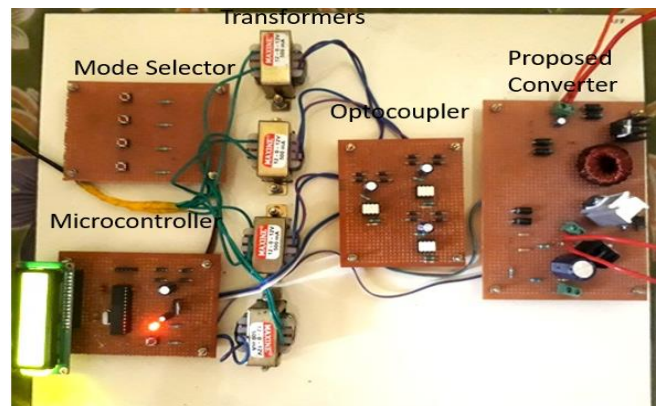


Figure 8 Hardware Prototype

In order to validate and verify the simulation results, a 200 W laboratory prototype of the proposed NI-TPBBC converter is built. The PV supply is mimicked using a Regulated Power Supply (RPS). The battery pack is made of 24 V/10 Ah rating with discharge capacity more than 3C for fast discharging. The switches, inductors, and capacitors are connected

Table 7 shows the comparison of the proposed NI-TPBBC converter with other converter topologies in terms of components, voltage gain, and features.

Table 7

CONVERTER IN REFERENCE	NUMBER OF ACTIVE SWITCHES	NUMBER OF DIODES	NUMBER OF INDUCTORS	NUMBER OF CAPACITORS	SWITCHING FREQUENCY	BIDIRECTIONAL/ UNIDIRECTIONAL	VOLTAGE EQUATION	VOLTAGE GAIN	REPORTED POWER RATING
[11]	4	2	2	3	100 kHz	Unidirectional	$V_o = d_1 V_{PV}$ $V_{bo} = (1 - d_2) V_o$	Low	400 W
[12]	8	0	2	1	20 kHz	Bidirectional	$V_o = \frac{V_b}{(1-D)}$	Medium	30 kW
[13]	3	1	1	3	50 kHz	Unidirectional	$\frac{1}{1-D}$	Medium	80 W
[14]	4	2	2	0	50 kHz	Unidirectional	$\frac{1}{1-D}$	Medium	2 kW
[15]	3	5	2	2	50 kHz	Bidirectional	$\frac{1+n}{1-D}$	High	300 W
[16]	4	2	2	1	20 kHz	Bidirectional	$D_i / (1-D)$	Low	1 kW
Proposed NI-TPBBC Converter	3	3	2	3	15 kHz	Bidirectional	$\frac{V_o}{V_{in}} = \frac{1+d}{1-d}$	High	250 W

The converter design in [13] consists of a similar number of components but it does not possess the feature of bidirectionality and has lesser voltage gain.

The topologies proposed in [11], [12], [14] all have a comparatively high number of switches leading to greater switching losses and are less compact.

The voltage gain of the proposed NI-TPBBC converter is higher when compared to other converter topologies. The reduced voltage stress and current stress in the proposed NI-TPBBC converter ensures lesser switching losses and facilitates the use of low rated components thereby decreasing the cost and providing a compact design. The multi-input feature in the proposed converter enables the integration of additional energy sources such as renewable energy. The bi-directionality is an added advantages making the design more energy-efficient and compatible with upcoming applications such as electric vehicles.

REFERENCES

[1] Danyali, Saeed, Seyed Hossein Hosseini, and Gevorg B. Gharehpetian. "New extendable single-stage multi-input DC-DC/AC boost converter." *IEEE Transactions on power electronics* 29.2 (2014): 775- 788.

according to the proposed design to obtain the Boost-Cuk topology. 50μF, 100μF capacitors, and 1mH inductors were used as C and L respectively. The switching frequency is set at 15kHz. The output was expected to be around 250 W.

Figure 8 shows the hardware prototype of the proposed NI-TPBBC Converter.

VI. CONCLUSION

A non-isolated dual-input Boost-Cuk converter topology has been proposed in this paper. The main advantages of the proposed converter are minimal design, simple control strategy, concurrent or independent power transfer capability of input ports, reduced number of components (switches, inductors, capacitors) and bidirectional power flow capability. Power regulation capability between the PV supply, battery and output is an advantageous property. The Converter as a design parameter has been extensively investigated and calculated for different input and load scenarios for all the modes of operation. The efficiency of the proposed topology has been verified by detailed analysis and experimental results. Hardware and simulation results validate the satisfactory working of proposed topology. The proposed converter can be capable of implementation in HEV/EV.

[2] Keyhani, Hamidreza, and Hamid A. Toliyat. "A ZVS single-inductor multi-input multi-output DC-DC converter with the step-up/down capability." In *Energy Conversion Congress and Exposition (ECCE)*, 2013 IEEE, pp. 5546-5552. IEEE, 2013.

- [3] Lee, Sin-Woo, and Hyun-Lark Do. "Isolated SEPIC DC-DC Converter with Ripple-Free Input Current and Lossless Snubber." *IEEE Transactions on Industrial Electronics*(2017).
- [4] Nguyen, Minh-Khai, Truong-Duy Duong, Young-Cheol Lim, and Yong Jae Kim. "Isolated Boost DC-DC Converter with Three Switches." *IEEE Transactions on Power Electronics* (2017).
- [5] Sayed, Mahmoud A., Kazuma Suzuki, Takaharu Takeshita, and Wataru Kitagawa. "New PWM technique for grid-tie isolated bidirectional DCAC inverter based high-frequency transformer." In *Energy Conversion Congress and Exposition (ECCE), 2016 IEEE*, pp. 1-8. IEEE, 2016.
- [6] Baek, Seunghun, and Subhashish Bhattacharya. "Analytical Modeling and Implementation of a Coaxially Wound Transformer with Integrated Filter Inductance for Isolated soft-switching DC-DC Converters." *IEEE Transactions on Industrial Electronics*(2017).
- [7] Hailong Zhang, *Student Member, IEEE*, Yafei Chen, *Student Member, IEEE*, Chang-Su Shin, Sung-Jun Park, and* Dong-Hee Kim, *Member, IEEE* "Transformerless Bidirectional DC-DC Converter for Battery Storage System with High Voltage Gain".
- [8] Kazem Varesi , Seyed Hossein Hossein, Mehran Sabahi, Ebrahim Babaei, Naser Vosoughi "Performance and design analysis of an improved non-isolated multiple input buck DC-DC converter". *IET Power Electronics*
- [9] Wu, Gang, Xinbo Ruan, and Zhihong Ye. "High Step-Up DC-DC Converter Based on Switched Capacitor and Coupled Inductor." *IEEE Transactions on Industrial Electronics*(2017).
- [10] Nejabatkhah, Farzam, Saeed Danyali, Seyed Hossein Hosseini, Mehran Sabahi, and Seyedabdolkhalegh Mozaffari Niapour. "Modeling and control of a new three-input DC-DC boost converter for hybrid PV/FC/battery power system." *IEEE Transactions on power electronics* 27, no. 5 (2012): 2309-2324.
- [11] Zihu Zhou, Hongfei Wu, Xudong Ma, Van Xingl " A Non-Isolated Three-Port Converter for Stand-Alone Renewable Power System".
- [12] Omar Hegazy†, Joeri Van Mierlo "Control and Analysis of an Integrated Bidirectional DC/AC and DC/DC Converters for Plug-In Hybrid Electric Vehicle Applications".
- [13] Mohammad Al-Soeidat* "A Reconfigurable Three-Port DC-DC Converter for Integrated PV-Battery System"
- [14] S. H. Hosseini, S. Danyali, F. Nejabatkhah, "Multi-input DC boost converter for grid connected hybrid PV/FC/Battery power system," in *Proc. IEEE EPEC*, Canada, Aug. 2010, pp. 1–6.
- [15] L. J. Chien, C. C. Chen, J. F. Chen, Y. P. Hsieh, "Novel Three-Port Converter With High-Voltage Gain," *IEEE Trans. Power Electron.*, vol. 29, no. 9, pp. 4693-4703, Sep. 2014.
- [16] F. Akar, Y. Tavlasoglu, E. Ugur, B. Vural, and I. Aksoy, "A bidirectional nonisolated multi-input DC-DC converter for hybrid energy storage systems in electric vehicles," *IEEE Trans. Veh. Technol.*, Vol. 65, No. 10, pp. 7944-7955, Oct. 2016.
- [17] H. Zhu, D. Zhang, B. Zhang, and Z. Zhou, "A nonisolated three-port dc-dc converter and three-domain control method for PV-battery power systems," *IEEE Trans. Ind. Electron.*, Vol. 62, No. 8, pp. 4937-4947, Aug. 2015.
- [18] M. Kumar, Y. N. Babu, D. Pullaguram, and S. Mishra, "A high voltage gain non-isolated modified three-port DC/DC converter based on integrated Boost-Cuk topology," in *2017 IEEE PES Asia-Pacific Power and Energy Engineering Conference (APPEEC)*, pp. 1-6, 2017.
- [19] P. KhademiAstaneh, J. Javidan, K. Valipour, and A. Akbarimajd, "Integrated bidirectional three-port DC-DC converter with ripple-free input current and soft switching," *J. Power Electron.*, Vol. 18, No. 5, pp. 1293-1302, Sep. 2018.
- [20] P. Zhang, Y. Chen, and Y. Kang, "Nonisolated wide operation range three-port converters with variable structures," *IEEE J. Emerg. Sel. Topics Power Electron.*, Vol. 5, No. 2 pp. 854-869, Jun. 2017.